CrossMark

ORIGINAL PAPER

Evaluation of natural quartz and zeolitic tuffs for As(V) removal from aqueous solutions: a mechanistic approach

F. Melak[1,5] · E. Alemayehu[2] · A. Ambelu[1] · E. Van Ranst[3] · G. Du Laing[4]

Abstract Naturally occurring pyroclastic materials, quartz-rich tuffs (Qz) and stellerite tuffs, were evaluated for their capacities to remove As(V) from aqueous solutions. The mechanism of As(V) uptake was evaluated using sequential extraction of As(V)-loaded adsorbent which entailed that the plausible removal mechanism is sorption to short-range ordered hydrous oxides of iron and aluminum. In addition, buffering effects of adsorbents could form favorable charges upon them through hydrolysis of amphoteric oxides, enhancing the performance of sorption. The influence of anions co-existing with As(V) in water such as carbonate, bicarbonate, nitrate, chloride, phosphate, and sulfate was studied in a batch sorption process. The impact of most anions on As(V) removal was found to be negligible except phosphate. The sorption behavior well fitted to Langmuir and Freundlich models. Estimated maximum sorption capacities of 0.42 and 0.23 mg/L were observed using quartz-rich tuffs and stellerite tuffs, respectively. As(V) concentration of 0.8 mg/L was easily decreased to below the drinking water standard of 0.01 mg/L using Qz adsorbent, whereas 0.1 mg/L As(V) decreased to below this limit upon the use of stellerite tuffs under similar conditions. The buffering capacity of quartz-rich tuffs and stellerite tuffs induced a pH increase to 5.76 and 5.40, respectively, from initial pH of 3.50, which will incur an important asset in real applications.

Keywords Arsenic · Quartz tuff · Sequential extraction · Sorption mechanism · Zeolitic tuff

✉ F. Melak
  fekadumelak95@gmail.com

1 Department of Environmental Sciences and Technology, College of Public Health and Medical Sciences, Jimma University, P.O. Box 378, Jimma, Ethiopia

2 School of Civil and Environmental Engineering, Institute of Technology, Jimma University, Jimma, Ethiopia

3 Department of Geology and Soil Science (WE13), Laboratory of Soil Science, Ghent University, Ghent, Belgium

4 Department of Applied Analytical and Physical Chemistry, Faculty of Bioscience Engineering, Ghent University, Coupure links 653, Ghent, Belgium

5 Department of Chemistry, College of Natural Sciences, Jimma University, Jimma, Ethiopia

Introduction

Pollution of groundwater and surface water by arsenic is largely due to the dissolution of minerals being naturally present (Amini et al. 2008). Moreover, anthropogenic activities such as combustion of fossil fuels and use of wood preservatives are among the potential sources of arsenic (Flora 2015). Arsenic in groundwater supplies above WHO guideline of 0.01 mg/L has been found in different parts of the world such as in Bangladesh (Smith et al. 2000), Vietnam (Berg et al. 2001), and Ethiopia (Getaneh and Alemayehu 2006; Rango et al. 2010). Ethiopia has abundant surface and groundwater resources of which groundwater takes the lion's share. However, over 10 million inhabitants of the Main Ethiopian Rift Valley (MER), who rely on groundwater for drinking and domestic applications, are exposed to naturally elevated arsenic levels, inducing health risks for the local population (Rango et al. 2013).

The variation in physicochemical properties such as pH, redox potential, and others often affect the environmental

Springer

fate of As: metal mobility, biological availability, and speciation (Manning and Goldberg 1996). As(V) and As(III) are most common in natural waters. As(V) predominates under normal conditions and causes major contamination of groundwater and surface waters (Xu et al. 2002). The global geogenic arsenic contamination prediction for groundwater and region-specific reports for MER aquifers mention As(V) in groundwater to be predominant over As(III) (Amini et al. 2008; Rango et al. 2013). Therefore, removal of As(V) is important regardless of the higher toxicity of As(III).

Sorption is one of the most promising and useful methods for removal of trace elements, including As. A wide range of possible adsorbents was reported for As(V) removal, for instance, alumina and iron-based adsorbents are very popular due to their high affinity for arsenate and arsenite, with greater resemblance in arsenate than arsenite (Xu et al. 2002; Mohan and Pittman 2007). However, the sorption mechanisms involved are insufficiently studied for most of the adsorbents, in general, and quartz tuffs and zeolitic tuffs in particular. Furthermore, consideration of naturally occurring and abundantly available adsorbents, as a replacement for high-cost adsorbents, is highly important in developing countries.

Tuffs are consolidated pyroclastic rocks. These rocks can form zeolite minerals (Hall 1998). Zeolitic tuffs commonly contain one or more zeolites, volcanic glass and other mineral phases as quartz, feldspar, calcite, and gypsum (Ruggieri et al. 2008). Various natural zeolites are found throughout the world, showing variability in composition from one location to another, and hence also variability in ion-exchange characteristics (Bogdanov et al. 2009), and a predictive variation in sorption efficiency. In Ethiopia, several million tonnes of zeolite deposits were discovered in rift valley sediments near *Nazret* and *Boru*, as well as in northern parts of Ethiopia, *Hashengie* and *Alagie* areas (Tadesse 2009; Gómez-hortigüela et al. 2014). Quartz is the second most abundant and widespread mineral in the Earth's surface characterized by specific properties ranging from point defects to macroscopic appearance which are dependent on the geological history and specific conditions of formation. Quartz contains numerous atoms out of place and various substitutional and interstitial impurities and defects. Some of these are inherently paramagnetic (e.g., Fe^{3+}) (Weil 1984). These mineral tuffs from Ethiopia: quartz and zeolite were employed to remove As(V) using batch system at Applied Analytical and Physical Chemistry Laboratory, Gent University, Belgium from September 2014 to June 2015.

Accordingly, the major objectives of the present work were to assess the potential of natural Qz and STL, from Ethiopia to remove As(V) from aqueous solutions and to reveal the sorption mechanism involved. Therefore, batch sorption experiments were conducted under different conditions and sequential extraction was performed on the As(V)-loaded adsorbents.

Materials and methods

Reagents

1000 mg/L As(V) stock solution was prepared by dissolving 4.165 g of Na2HAsO4·7H2O (Sigma Aldrich) in a liter of deionized water (resistivity >18.2 MΩcm). Solutions used in the experiments were freshly prepared through subsequent dilutions. Separate working solutions containing As(V) concentrations of 0.05, 0.1, 0.2, 0.4, 0.8, 1.6, 3.2, 6.4, 12.8, and 25 mg/L for Qz adsorption tests and 0.05, 0.1, 0.2, 0.4, 0.8, 2, and 4 mg/L for STL were prepared in a deionized water. As(V) stock solution was stored at 5 ± 1 °C in polyethylene plastic bottles to prevent speciation changes. In such conditions, arsenic is stable for three months as indicated in the literature (Hall et al. 1999). 0.1 M HCl and 0.1 M NaOH were used for pH adjustments. pH of the solution was monitored prior to and after each sorption using a digital pH meter (ORION star A211). Sodium salts of nitrate, sulfate, chloride, phosphate, carbonate, and bicarbonate were used for the experiments in studying the effect of co-existing ions.

Adsorbent processing and characterization

In this study, Qz and STL were obtained from *Hashengie*, Ethiopia. The collected samples were washed several times with deionized water after each stage of grinding and dried. The adsorbents were ground and sieved by a ASTM E-11 Laboratory Test sieve of 300 μm mesh size. The adsorbents were identified using XRD patterns of fine grinded powder samples recorded on a Bruker D8 ECO equipped with a Cu tube anode and the Lynxeye XE energy-dispersive position sensitive detector. The incident beam was automatically collimated. The tube was operated at 40 kV and 25 mA, and the XRD data were collected in a θ, 2θ geometry from 3.00° onwards, at a step of 0.010° 2θ, and a count time of 48 s per step. Concentrations of constituent elements of both adsorbents, Qz and STL, were measured in duplicate using ICP-OES (VISTA-MPX CCD Simultaneous Varian version 2.0) after microwave-aided acid digestion according to EPA method 3052 (Da Silva et al. (Da Silva et al. 2014)). Therefore, 0.5 g well-mixed adsorbents and a CRM (certified reference material, for quality control) were weighed accurately in Teflon vessels. Subsequently, 9 ± 0.1 mL concentrated nitric acid and 4 ± 0.1 mL concentrated hydrochloric acid were added to the Teflon vessel in a fume hood. After 1 h, 4 ± 0.1 mL

concentrated hydrofluoric acid was added to the mixture. Then, it was digested in a microwave oven at a temperature of 200 °C, a pressure of 500 psi, and a power of 1000 W for 20 min, with these conditions being reached in 15 min. Subsequently, 40 mL of a 4% (w/v) solution of boric acid was introduced into the solution to safeguard the ICP-OES from fluoride of hydrofluoric acid. Finally, the suspension was filtered over acid-resistant 0.45-μm filters (Whatman 542, Whatman International Ltd) in 100-mL plastic flasks and then filled to the mark using deionized water. These filtrates were analyzed using ICP-OES.

Determination of Pzc

The point of zero charge was estimated by using a batch equilibrium technique described by Borah and Senapati (Borah and Senapati 2006). For this, 50 mL of 0.1 M NaNO$_3$ (Merck, Darmstadt, Germany), i.e., a solution of inert electrolyte, was prepared and initial pH values were adjusted from 2.5 to 12, in intervals of 0.5. The introduction of small amounts of concentrated inert electrolyte causes a shift of pH toward Pzc, whereas no shift is observed at Pzc (Kallay 2000). Thus, 1 g of each adsorbent was added to the pH-adjusted electrolyte solutions and shaken for equilibration. Then, the solutions were filtered and final pH values were recorded. By plotting the initial pH values versus the solution pH at equilibrium, Pzc of the adsorbents could be obtained from the plateau of constant pH.

Surface area and bulk density determination

An aliquot of 0.5 g each adsorbent was poured into 50 mL solutions containing 150 mg/L methyl blue in volumetric flasks. Solutions were shaken to equilibrate. Afterward, the amount of methyl blue solution remained as supernatant was determined using a Jenway 6400 Spectrophotometer set at 663 nm (İnel and Tümsek 2000). The adsorbed amount of methyl blue concentration was calculated from the difference between initial and equilibrium concentrations. For bulk density determination, a graduated 25-mL glass cylinder was weighed (W_1). The weight of the adsorbents (dried at 105 °C for 12 h) filled to the mark plus the cylinder was recorded as W_2. The weighed adsorbents were moistened so as to fill the void spaces within the adsorbent, keeping the volume not greater than the mark of the cylinder (25 mL), and the cylinder was weighed again (W_3). Finally, the bulk density was calculated as: $W_3 - W_1/25$ mL.

Batch sorption experiments

The batch sorption process was undertaken using a horizontal GFL shaker (memmert, D-30938, Germany).

Equilibrium solution was collected by a syringe and filtered over a Millipore Chrome AFiL RC-4/25 membrane filter with pore size of 0.45 μm. The filtrate was then analyzed for total amount of arsenic using ICP-MS (PerkinElmer Sciex, ELAN DRC-e) that remained unsorbed. The instrument was set with conditions of: power 1600 W, dwelling time 200 ms, sweeps/reading 3–20, arsenic mass As 75, and adjusted to take readings in replicates of three and averaging. 10 ppb Ga-Rh internal standard was used to correct for non-spectral interferences. The batch sorption experiments were performed in triplicate, and the average results were reported, together with error bars based on standard deviation of the triplicate.

Effect of contact time

The effect of contact time was studied in an experiment conducted at a pH of 6.50, below Pzc of adsorbents. In this experiment, 10 g/L of each adsorbent was added to 25 mL of 2 mg/L As(V) solutions. Then, suspensions were shaken at room temperature for time intervals from 30 min to 30 h. The resulting suspensions were analyzed for its As concentration according to the procedure described in Sect. 2.3.

Effect of pH

The effect of solution pH was investigated to determine the optimum pH for As(V) removal. The initial pH was studied in the range 3.00–11.50. A dose of 10 g/L adsorbents and 2 mg/L of As(V) aqueous solution adapted to a desired pH value was used in the process. The resulting suspensions were also analyzed for its As concentration following the procedure described in Sect. 2.3.

Adsorbent dose evaluation

The effect of the adsorbent dose was studied in ranges 4–80 g/L to evaluate most economical and optimal dose for each adsorbent. In order to obtain the sorption efficiency (%ε) and capacity, the amount of ions adsorbed was calculated with the following equations:

$$\%\varepsilon = \frac{c_0 - c_e}{c_0} \times 100 \tag{1}$$

$$q_e(t) = \frac{(C_0 - C_e(t))V}{m} \tag{2}$$

where q_e is the amount of As(V) removed from solution (mg/g); C_0 is initial concentration of As(V) in solution before mixing with adsorbent (mg/L); C_{eq} is the

equilibrium concentration of As(V) left in the solution (mg/L); V is the solution volume (L), and m is the weight of adsorbent in gram (g).

Desorption study

To evaluate regenerability of the adsorbents, NaOH (0.1 M) and betaine (0.01 M) solutions were used in the desorption experiments. Initially, the adsorbents were treated with 2 mg/L As(V) solution setting the solution at optimal conditions (pH 3.50, dose 20 g/L, 25 °C, 200 rpm, and 24 h). After sorption, the suspensions were centrifuged at 9800 rcf for 1 min using an Eppendor 5804R centrifuge (Eppendorf AG, Hamburg). Adsorbents were separated by decantation and dried at 70 °C for 24 h. Desorption was conducted by shaking the As(V)-loaded adsorbents under similar conditions as sorption step, except the pH. The desorbed amount of As(V) was determined in the supernatant solution after filtration over a 0.45-μm membrane filter.

Sequential extraction: a case of Qz adsorbent

Ten adsorbent samples of 1 g each Qz, five of them loaded with 0.0824 mg/g As(V) at pH 3.50 and five loaded with 0.0325 mg/g at pH 7.00, were extracted with a five-step sequential extraction procedure adopted from Wenzel et al. (2001). In this procedure, subsequent extractions were conducted on the solid residues collected after centrifugation in each consecutive extraction step. Thereafter, 1 g of each adsorbent loaded with As(V) was placed in a 45-mL centrifugation tube and 25 mL of each extraction reagent was subsequently added in order of increasing extraction strength as follows: (1) 0.05 M $(NH_4)_2SO_4$ shaken at 200 rpm at a temperature of 20 °C for 4 h; (2) 0.05 M $NH_4H_2PO_4$ shaken at 200 rpm at a temperature of 20 °C for 16 h; (3) 0.2 M NH_4^- oxalate buffer, pH 3.25, shaken at 200 rpm in the dark at 20 °C for 4 h; (4) 0.2 M NH_4-oxalate buffer + ascorbic acid, pH 3.25, heated in a water bath at 96 °C for 30 min and (5) microwave-assisted digestion using HNO_3/H_2O_2. For the latter HNO_3/H_2O_2 extraction, 8 mL of 65% HNO_3 and 4 mL of 30% H_2O_2 were added to the residue of the previous extraction step, followed by microwave digestion at a pressure of 34.02 psi, a temperature of 200 °C, a power of 1000 W, and with a raise time of 20 min and hold time of 15 min (Mketo et al. 2015). After each extraction step, the tubes containing the samples were centrifuged at 3000 rcf for 5 min. Then, from each extracted solution, part of the solution to be used for arsenic analysis was collected using a syringe and filtered using a 0.45 μm Millipore Chrome AFiL RC-4/25 membrane filter. The remaining solution was carefully decanted to collect the solid residue for the next extraction step (Fig. 1).

Results and discussion

Physicochemical characterization of the adsorbents

In characterizing the adsorbents, XRD pattern was compared with patterns of references, which revealed the identity of each mineral present in the sample. The XRD pattern was compared with patterns of references, which revealed the identity of each mineral present in the sample. In one of the adsorbents, referred to as stellerite tuff (STL), almost all peaks of the XRD pattern were matched with stellerite (Fig. 2a). The second adsorbent, referred to as quartz tuff (Qz), is almost completely composed of quartz, and minor amounts of feldspar, diopside, traces of stilbite and stellerite (Fig. 2b). Moreover, elemental composition analysis revealed the presence of iron and aluminum (Table 1).

Effect of contact time on sorption

The dependence of As(V) sorption on contact time is illustrated in Fig. 3. The sorption capacities increased with increasing contact time until the state of equilibrium. In this experiment, the removal stabilized after 24 h. Therefore, 24 h was chosen as contact time for both adsorbents in further experiment. It was observed that relatively faster sorption removal of As(V) was achieved by both adsorbents up to 12-h exposure. Afterward, the number of active sorption sites gradually decreased due to which the sorption process became slow.

Point of zero charge (Pzc)

The Pzc of Qz and STL adsorbents was found to be 7.38 and 6.99, respectively. This lays within the range of Pzc values of oxides of α-Al_2O_3 of corundum, α-Fe_2O_3 of hematite, and Fe_3O_4 of magnetite which is in the range (6.6–9.1) (Brown et al. 1999). The effective point of zero charge values for solid matrices differ from reported for pure oxide minerals (Taubaso et al. 2004). The pH after sorption was found to range from 5.76 to 6.78 and from 5.40 to 6.00 for Qz and STL adsorbents, respectively, which actually is near the point of zero charge, indicating the high buffering capacity of both adsorbents.

Effect of solution pH and redox potential

Oxidation–reduction potential (ORP) and pH can control environmental forms of arsenic. Thus, to better describe which arsenic species involved in the sorption process, pH of equilibrium solution and ORP were monitored. Based on the measured solution pH at equilibrium and redox
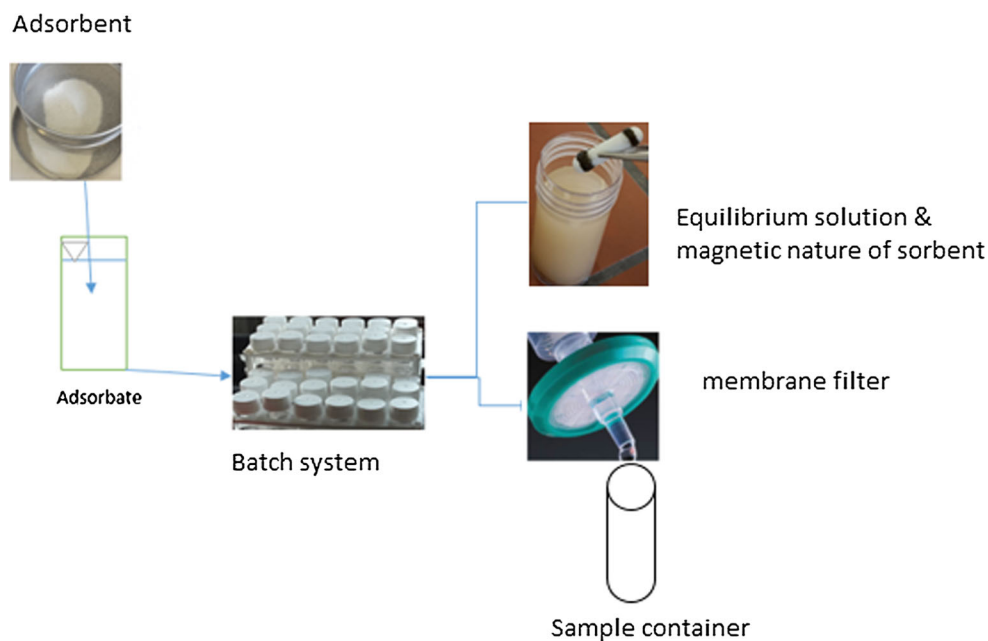
Fig. 1 A scheme of experimental setup to study batch sorption of As(V) using Qz

potential, each arsenic form was estimated using visual MINTEQ 3.1 chemical equilibrium model. Arsenic forms predicted by monitoring the pH at equilibrium as function of ORP from the initial working As(V) solution are illustrated in Fig. 4 and Table 2. The results explained that the ORP decreased from 357 mV to 200 mV when pH increased from 3.00 to 6.80, indicating $H_2AsO_4^-$ form of As(V) predominates, whereas in pH range of 6.8–12, $HAsO_4^{2-}$ of As(V) occurred as major entity. From nearly pH 12 afterward, AsO_4^{3-} was shown to dominate, inducing a reduced condition. In general, $H_2AsO_4^-$ was found to be the primary constituent of As(V) in the experimental conditions. The occurrence of dominant species of arsenic in solution as function of both parameters (pH and ORP) was well documented. For instance, at higher redox levels (500–200 mV) and at low pH (less than about pH 6.9), 65–98% of arsenic in solution was present as As(V) (Masscheleyn et al. 1991; Mohan and Pittman 2007). More specifically, these results were well in agreement with reports: $H_2AsO_4^-$ was predominant in pH 2–7, $HAsO_4^{2-}$ in the range of pH 7-12, and AsO_4^{3-} in pH 12-14 (Shevade and Ford 2004; Chutia et al. 2009a).

The influence of solution pH for As(V) removal and buffering effect of adsorbents is presented in Fig. 5 and 6. It could be noted that both adsorbents removed As(V) effectively over the initial pH range of 3–6. The high removal of As(V) under acidic conditions could be due to columbic attraction of As(V) oxyanions of As(V) with adsorbents active sites (Xu et al. 1988, 2002). The decrement in the removal of As(V) at higher

pHs ≈ 6.2 afterward is attributed to the increase in number of negatively charged sites on the surface of the adsorbents. Thereafter, the enhanced electrostatic repulsion plus the potential competition of As(V) oxyanions with hydroxyl ions to the surface should be responsible for the decrease in the removal of As(V) observed under alkaline conditions.

The buffering effect of adsorbents which could be explained by the amphoteric nature of oxides of adsorbent surfaces was noticed during sorption process. Thus, at low pH, the hydrolysis equilibria of amphoteric oxides of Qz and STL shift toward the left (to the cationic surface of sorbents) increasing the bulk solution pH, whereas at high initial pH (pH > Pzc), the surface acid dissociation shift becomes the governing factor which causes a decrease in the bulk solution pH. The buffering effect of Qz was found to be higher than STL which actually was shown to be in line with the sorption capacities of adsorbents. Such buffering effect on sorption was also demonstrated in the use of natural iron ores (Zhang et al. 2004) and zeolite sorbents as to possess high As(V) sorption capacity due to the buffering nature (Shevade and Ford 2004). It was also indicated that the buffering capacity of the adsorbents could be explained by the presence of Si, Al, and Fe oxides that are amphoteric in nature (Li et al. 2012). Remarkably, the responsible mechanism of As(V) removal was supposed to be affected by the processes to gain the final pH of the solution from the initial set. This was most likely from the formation of favorable surface charges onto short-range ordered and hydrous oxides of iron, silicon, and aluminum
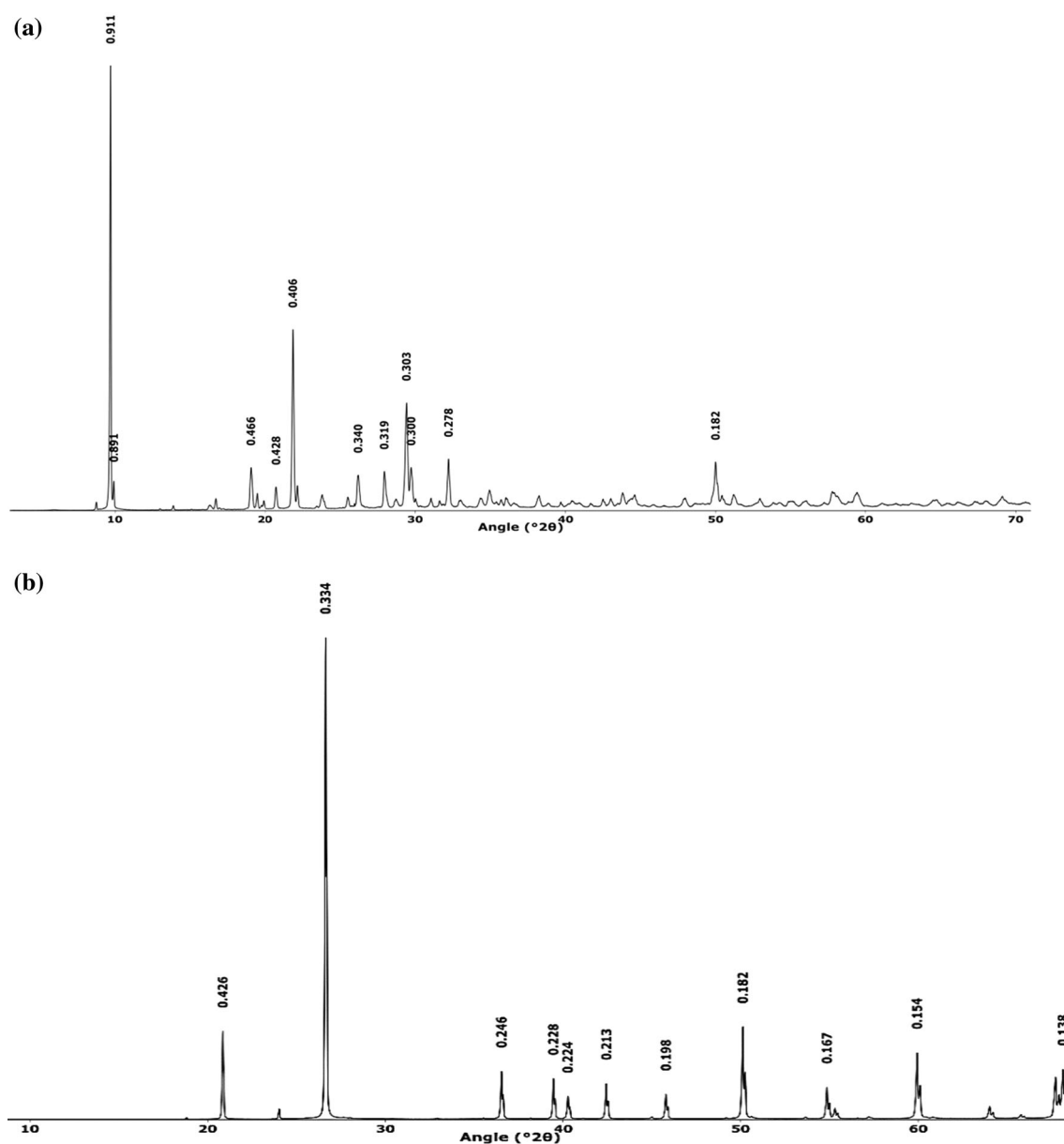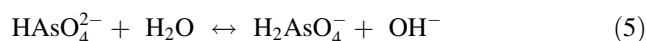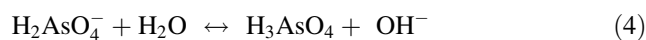
Fig. 2 XRD patterns of the adsorbents: **a** STL and **b** Qz

groups of Qz and STl tuffs. The stated mechanism of sorption has been in agreement with the results of sequential extraction of As(V) in case of Qz (Fig. 7). Hydrous oxides of iron and aluminum have strong affinity for As(V) oxyanions, expected to be due to ligand exchange and inner-sphere complexation reactions (Wenzel et al. 2001; Sverjensky and Fukushi 2006; Ayoob and Gupta 2009; Fufa et al. 2014; Kim et al. 2014). Moreover, it is evidenced that Fe and Al (hydr)oxides bearing adsorbents are efficient in As(V) removal processes (Fuller et al. 1993; Katsoyiannis and Zouboulis 2004). Thus, the plausible mechanisms involved Eqs. (8) and (9) in the sorption of As(V), and the behavior of adsorbate and

adsorbent species in the aqueous solution Eqs. (3–7) can be proposed.

At pH < pHzc (working condition):

$$H_3O^+ + HAsO_4^{-2} \leftrightarrow H_2AsO_4^- + H_2O \tag{3}$$

$$H_2AsO_4^- + H_2O \leftrightarrow H_3AsO_4 + OH^- \tag{4}$$

$$HAsO_4^{2-} + H_2O \leftrightarrow H_2AsO_4^- + OH^- \tag{5}$$

Further, considering the adsorbent at both basic and acidic conditions:

$$\equiv MOH_2^+ \leftrightarrow \equiv MOH + H^+ \tag{6}$$

$$\equiv MOH \leftrightarrow MO^- + H^+ \tag{7}$$
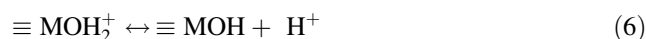
Table 1 Physicochemical properties of the studied sorbents

Adsorbents	Qz	STL
Si (wt%)	27.006	33.013
Al (wt%)	0.089	5.449
Fe (wt%)	0.947	0.547
Ca (wt%)	0.078	4.349
Mg (wt%)	0.036	0.067
K (wt%)	0.053	0.100
Na (wt%)	0.228	0.123
pH in water	7.81	8.19
Pzc	7.38	6.99
Surface area (m^2/g)	20.0	35.5
Bulk density (g/cm^3)	1.88	1.03
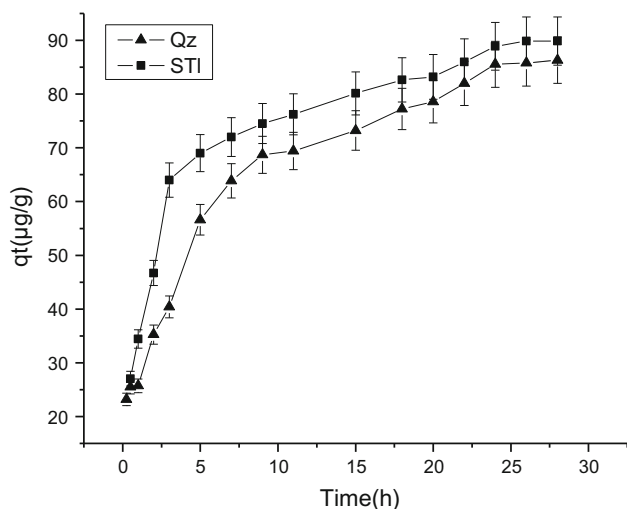
Fig. 3 Effect of contact time on As(V) removal (conditions: initial As concentration 2 mg/L, temperature 25 °C ± 2, adsorbent dose 10 g/L, solution pH 6.50, and agitation speed 200 rpm)

$$\equiv MOH_2^+ + H_2AsO_4^- \leftrightarrow MOH_2 — H_2AsO_4 \qquad (8)$$

$$\equiv 2MOH_2^+ + HAsO_4^{-2} \leftrightarrow (MOH_2)_2 — HAsO_4 \qquad (9)$$
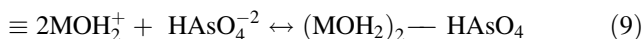
where M might be Si, Al, and Fe.

Sequential extraction: examining mechanism of sorption

To further investigate the mechanism of As(V) sorption, sequential extraction on Qz adsorbent loaded with As at pH 3.50 and 7.10 was conducted according to Wenzel et al. (Wenzel et al. 2001). The results showed that As(V) is primarily associated with the NH_4 oxalate buffer extractable fraction (65.52%) when the adsorbent was loaded at pH 3.50, pointing toward the short-range ordered and hydrous oxides of iron and aluminum being the major causes of sorption. The $(NH_4)H_2PO_4$ fraction (32.41%) indicated arsenic being specifically sorbed onto the surface of the adsorbent (Qz) (Fig. 7). Only few arsenic is found in the NH_4-Oxalate buffer + ascorbic acid $(NH_4)_2SO_4$ extractable and residual phases for As(V)-loaded sorbent at pH 3.50. Similar mechanisms were involved when the adsorbent was loaded with As(V) at pH 7.10. Fractionation profiles were similar compared to the profiles of adsorbent loaded at pH 3.50, except that a relatively smaller fraction of As(V) was shown in $(NH_4)_2PO_4$ extractable, but more As(V) (86%) remained in the NH_4-oxalate buffer extractable fraction. Next to NH_4-oxalate buffer extractable fraction, $(NH_4)_2PO_4$ was the one entailing presence of specific inner-sphere surface complexes as mechanism in the sorption process.

During the sequential extraction analysis, the validity of the data (precision and accuracy) was estimated for both groups of samples loaded by sorption at pH 3.50 and 7.10. Precision (closeness among each data points), in this case explained using coefficient of variation (CV), was calculated and found to be below 5% for fractions 1 to 5 made in the sequential extraction of five replicates. The percent error estimated to explain accuracy of the method and obtained from the formula: ((amount of As(V) initially adsorbed in the given mass of adsorbent (as a true value)-(pseudo) total amount from the sum of each fractions of arsenic)/amount of As(V) initially adsorbed in the given mass of adsorbent)) × 100% was found ≈ 6%. These cases indicated reasonable precision and accuracy of the method.

Effect of adsorbent dose

The effect of the adsorbent dose (4–80 g/L) was studied to evaluate the optimal and most economical amount of adsorbent. As(V) sorption at varying adsorbents dose is presented in Fig. 8a, b. The sorption efficiency of As(V) showed to increase with increasing adsorbents dose. The increase in the sorption efficiency with an increase in the adsorbent dose can be attributed to the increase in the number of active sorption sites. In the study, for a fixed concentration of As(V) used (2 mg/L), As(V) removal efficiency did not show significant change above an adsorbent dosage of 20 g/L. Therefore, 20 g/L adsorbent was used for subsequent sorption process. Alternatively, As(V) sorption capacities decreased with an increase in adsorbent dose of 10 g/L afterward. Such decrement in sorption capacity is attributed to the fact that As is diluted over the surface of the adsorbent when the amount of adsorbent is further increased.
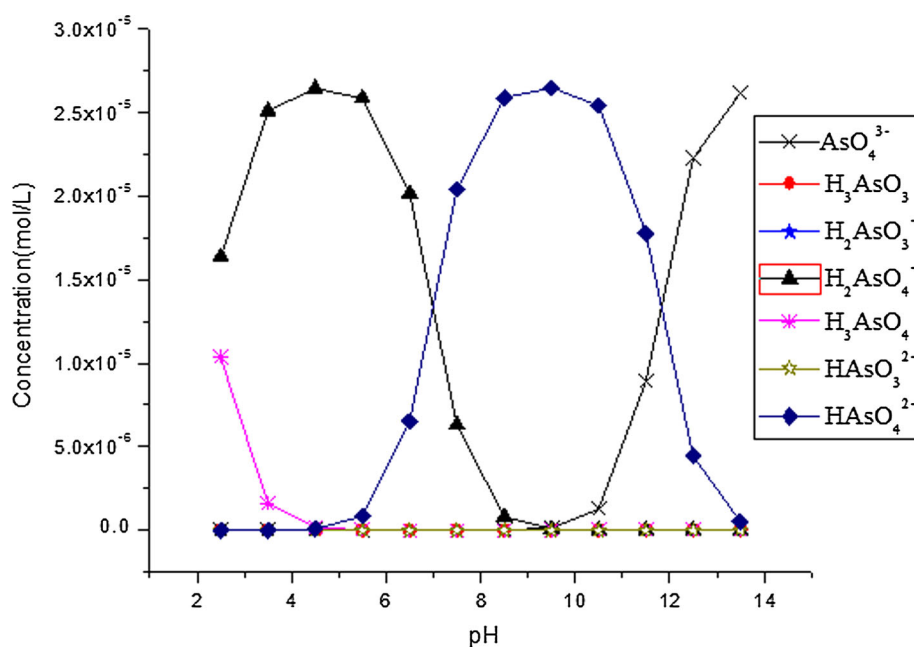
Fig. 4 Theoretical prediction of arsenic species using visual MINTEQ 3.1 from measured OPR (350 mV) and pH at 25 °C

Table 2 Prediction of arsenic species using visual MINTEQ 3.1 from measured ORP and pH (conditions: initial 2 mg/L As(V) and 25 °C)

| pH	ORP (mV)	Concentration (mol/L)						
		AsO_4^{-3}	H_3AsO_3	$H_2AsO_3^-$	$H_2AsO_4^-$	H_3AsO_4	$HAsO_3^{-2}$	$HAsO_4^{-2}$
3.5	**350**	4.071×10^{-17}	1×10^{-16}	2.138×10^{-22}	2.510×10^{-5}	1.584×10^{-6}	5.370×10^{-33}	8.123×10^{-9}
4.5	**239.3**	2.249×10^{-14}	9.999×10^{-17}	4.898×10^{-21}	2.643×10^{-5}	7.278×10^{-8}	2.8182×10^{-30}	1.959×10^{-7}
6.5	**200**	3.271×10^{-11}	9.979×10^{-17}	2.133×10^{-19}	2.017×10^{-5}	1.273×10^{-9}	5.359×10^{-27}	6.526×10^{-6}
7.28	**156**	5.329×10^{-10}	9.873×10^{-17}	1.272×10^{-18}	9.049×10^{-6}	9.476×10^{-11}	1.925×10^{-25}	1.765×10^{-5}
8.18	**140**	6.314×10^{-9}	9.032×10^{-17}	9.678×10^{-18}	1.550×10^{-6}	1.951×10^{-12}	1.218×10^{-23}	2.514×10^{-5}
9.23	**58**	6.648×10^{-8}	4.827×10^{-17}	5.173×10^{-17}	1.632×10^{-7}	2.054×10^{-14}	6.512×10^{-22}	2.647×10^{-5}
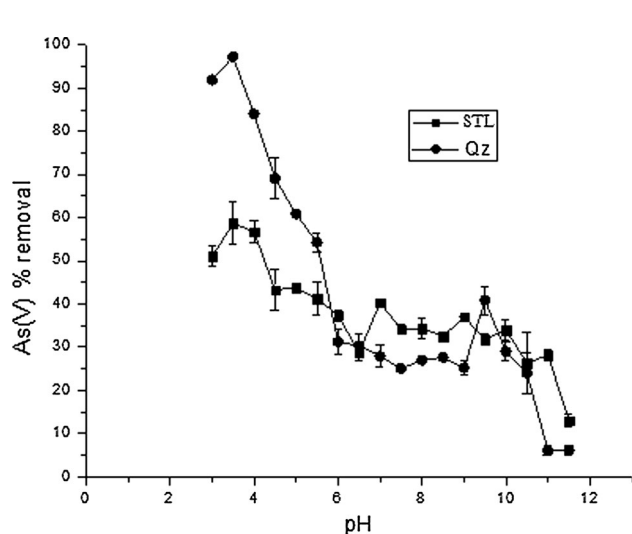
Fig. 5 Effect of pH on the removal of As(V) (conditions: temperature 25 ± 2 °C, adsorbent dose 10 g/L, concentration 2 mg/L As(V), time 24 h, and shaking speed 200 rpm)
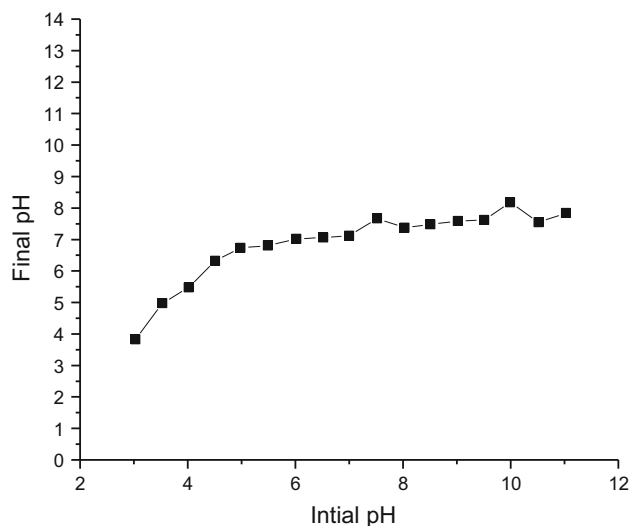

Fig. 6 Impact of A(V) sorption on pH of the solution (2 mg/L As(V), Qz adsorbent dose 10 g/L, contact time 24 h, temperature 25 ± 2 °C, and shaking speed 200 rpm)
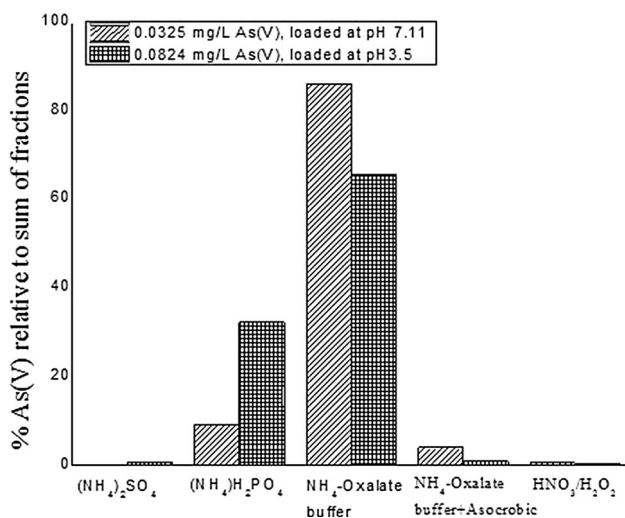
Fig. 7 Sequential extraction of As(V) from loaded sorbent (Qz)

Effect of initial As(V) concentration

The adsorption capacities of both adsorbents, Qz & STL, increased with an increase in initial As(V) concentrations (Fig. 9a, b). It was observed that an As(V) concentration of 0.8 mg/L at an adsorbent dose of 20 g/L Qz decreased to below 0.01 mg/L using Qz, whereas the initial As(V) concentration cannot exceed 0.1 mg/L when the aim is to push the As(V) concentration below 0.01 mg/L, the WHO standard for As in drinking water, using STL under the same operation conditions. The capacities of selected similar adsorbents for sorption of As(V) are summarized in Table 3.

Adsorption isotherms

The empirical isotherm models (Langmuir and Freundlich) are valid only for the chemical conditions under which the experiment was conducted. Langmuir model is based on the assumptions that the adsorbate is adsorbed on a fixed number of active sites, all being energetically equivalent, and with no interaction between the ions (Langmuir 1918). The Freundlich isotherm model is usually used in special cases of heterogeneous surface energy characterized by the heterogeneity factor $1/n$. The nonlinear forms of Langmuir and Freundlich isotherms are given by the following equations:

$$\text{Langmuir}: q_e = q_{max}bC_e/(1 + b * C_e) \tag{10}$$

$$\text{Freundlich}: q_e = k * C^{(1/n)} \tag{11}$$

The nonlinear Langmuir and Freundlich sorption plots for the equilibrium adsorption of As(V) on both Qz and

STL are presented in Fig. 10. The maximum adsorption (qmax) was estimated to be 0.42 and 0.23 mg/g for Qz and STL for the studied concentration ranges, respectively. The sorption capacity of STL is lower than Qz under the same experimental conditions.

Langmuir model (adjusted $R^2 = 0.987$) could be fitted better for Qz compared to the Freundlich model (adjusted $R^2 = 0.915$), whereas STL sorbent could be fitted well to both Langmuir and Freundlich model, with adjusted R^2 values of 0.992 and 0.999, respectively. This might infer more As(V) specific sorption upon the surface of Qz compared to STL. The nature of favorability of adsorption can be predicted by evaluating the dimensionless constant, separation factor(RL); RL = 1/(1 + bC0)(Weber and Chakravorti 1974), where C_0 (mg/L) is the initial As(V) concentration and b (L/mg) is the Langmuir constant. During adsorption in the use of Qz, the RL value computed for As(V) was found in range of 0.007–0.786 for concentration ranges of 25 mg/L to 0.05, with decreasing RL values at high initial concentrations. The values of RL were found within the range 0 < RL < 1, signifying favorable equilibrium adsorption of As(V).

Influence of co-existing ions on As(V) sorption

The impact of the presence of anions expected to occur together with As in water networks, including chloride, carbonate, bicarbonate, nitrate, sulfate, and phosphate, on the removal of As(V) was investigated, and results are illustrated in Fig. 11.

Chloride, sulfate, bicarbonate, and nitrate present in common concentration ranges showed negligible influence on As(V) removal, whereas phosphate reduced As(V) removal by competing with arsenic for active sites. This phenomenon has been elucidated by several other authors with similar sorbents (Chowdhury and Yanful 2010; Shan and Tong 2013). Phosphate and arsenate are both inner-sphere complex-forming oxyanions, which behave similarly on their mechanism of sorption on the adsorbent surface (Zhu et al. 2009). Similar effects on arsenic sorption were previously observed in the presence of phosphate when using natural iron ores, while only slight effects were noted in the presence of sulfate and chloride (Zhang et al. 2004). At equal concentrations, phosphate in soil outcompetes arsenate for adsorption sites because of its smaller size and higher charge density (Wenzel et al. 2001). However, phosphate is absent or usually present at lower concentration levels, e.g., 0.21 mg/L, in ground waters
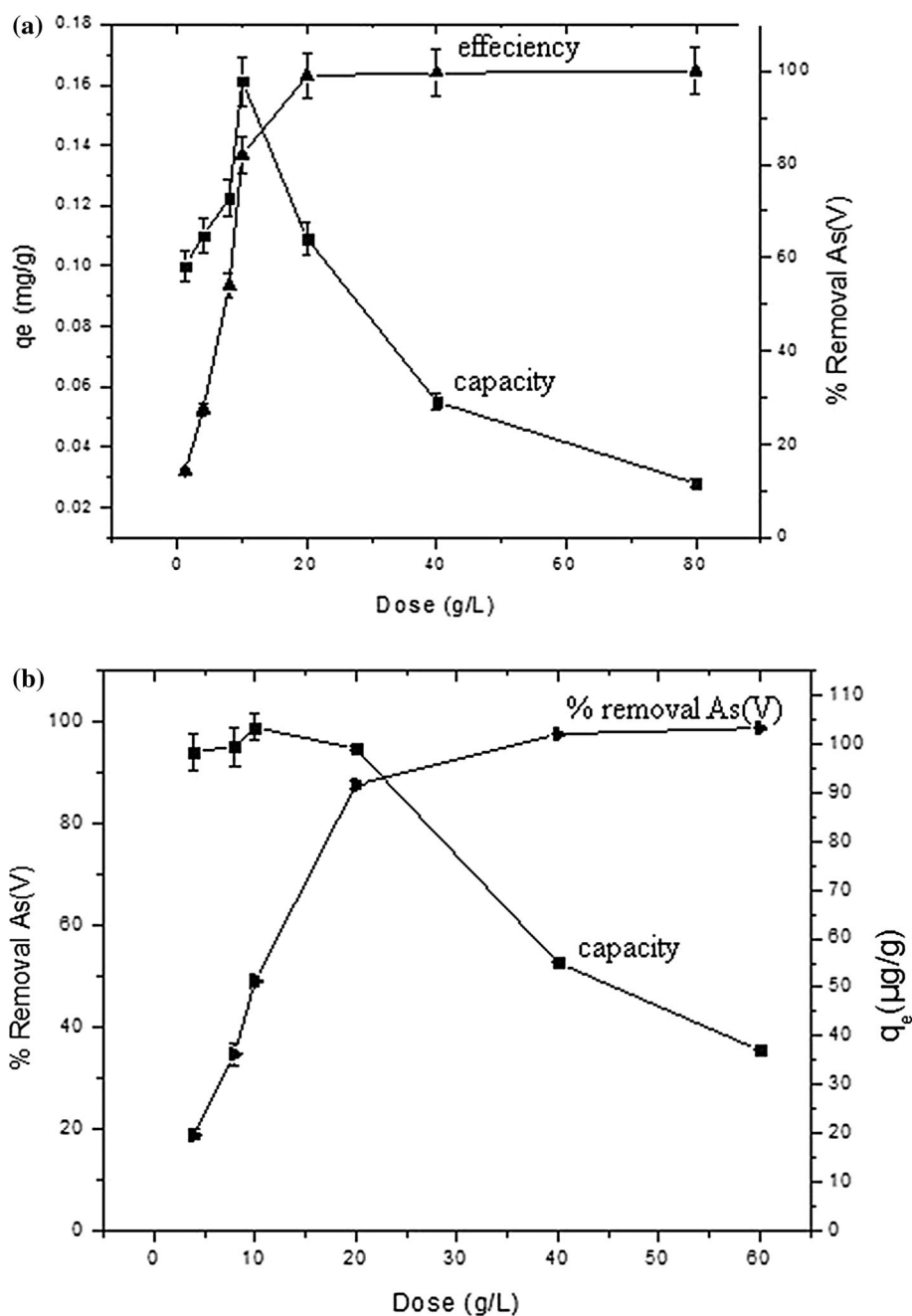
Fig. 8 Effect of adsorbent dose on the removal of As(V) using Qz (**a**) and STL (**b**) adsorbents (conditions: initial As(V) concentration 2 mg/L, temperature 25 ± 2 °C, pH 3.5, equilibrium time 24 h, and shaking speed 200 rpm)

of Ethiopia (Rango et al. 2010; Fufa et al. 2013). It was also reported that phosphate and arsenate followed similar trends on pH-based speciation. Phosphate within pH range of 2.5–7 (experimental condition) was reported as $H_2PO_4^-$ species which indeed have similar charge and behavior with $H_2AsO_4^-$(Zeng 2004).

Desorption study

0.1 M NaOH and 0.01 M betaine solutions were used in the desorption experiment. Nearly 67 and 63% of the adsorbed As could be desorbed when using 0.1 M NaOH and 0.01 M betaine, respectively. Thus, more than one desorption step
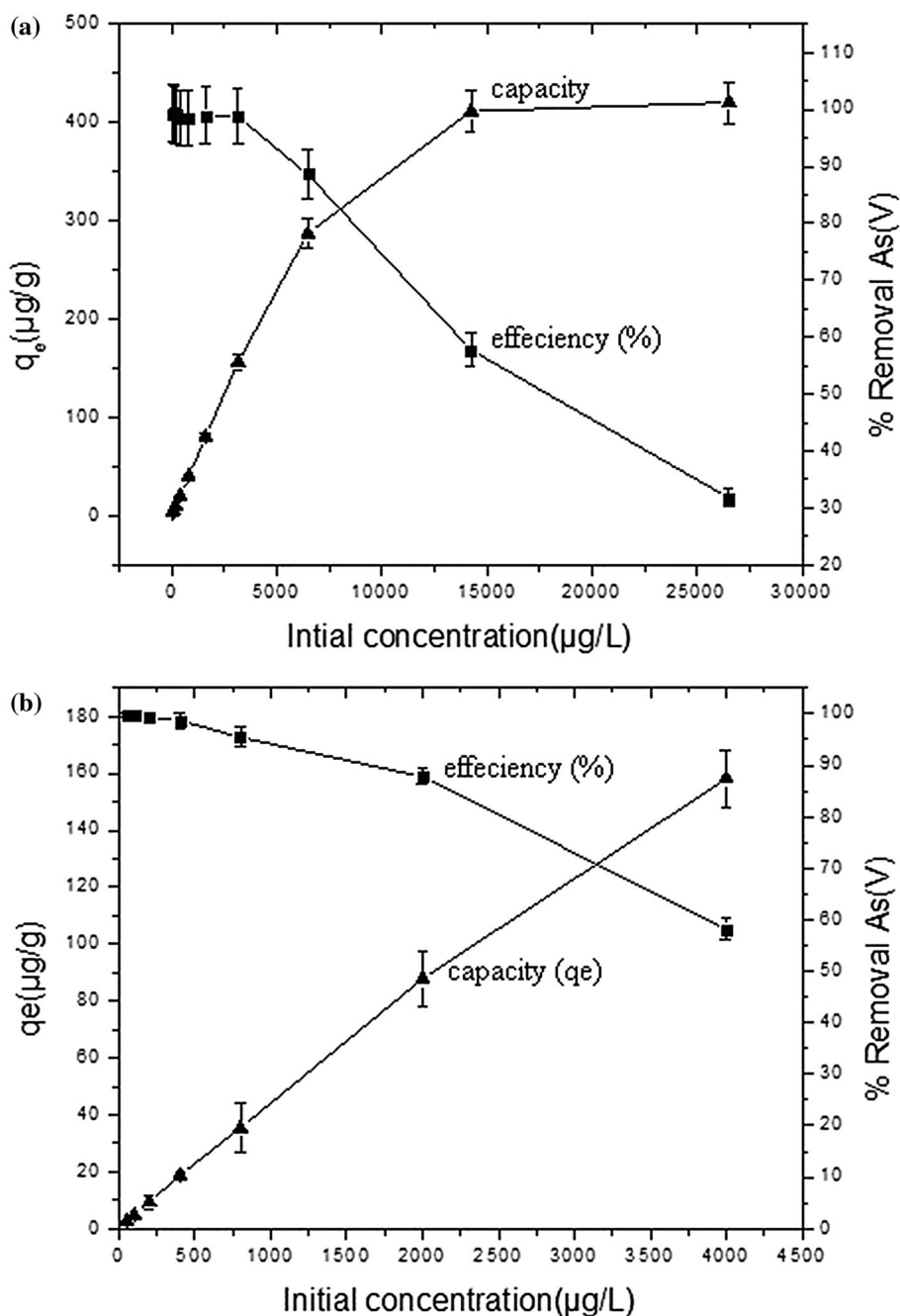
Fig. 9 As(V) removal efficiency and sorption capacities of Qz (**a**) and STL (**b**) as function of As(V) concentration (conditions: temperature 25 ± 2 °C, adsorbent dose 20 g/L, solution pH 3.50, equilibration time 24 h, and shaking speed 200 rpm)

seem to be required for complete desorption. In addition, high adsorption efficiency was considered at initial pH of 3.50; therefore, pH adaptation remains essential though the buffering capacity of adsorbents plays an important role in bringing near to pH 6, after sorption process. Further work may focus on modifying the adsorbents, as well as upscaling the system to investigate the applicability of the adsorbents on field scale.

Conclusion

Ethiopian quartz-rich tuffs (Qz) and stellerite tuffs (STl) were very effective adsorbents for removal of wide concentration levels of As(V) which is expected to occur in ground and surface waters. Qz and STL reduced As(V) concentrations to below the WHO's guideline values from initial concentrations of 0.8 and 0.1 mg/L

Table 3 Summary of sorption capacities of some selected adsorbents

Type of adsorbents	Removal capacity (mg/g)	Ratio of (S/L)	pH	Reference
Natural mordenite	1.299	1 g/100 mL	<4.2,	(Chutia et al. 2009b)
Natural clinoptilolite	0.699	1 g/100 mL	<5.2	(Chutia et al. 2009b)
Natural iron ores	0.4	0.5 g/100 mL	4.5–6.5	(Weber and Chakravorti 1974)
Hematite	0.202		2–8	(Guo et al. 2007)
Biotite	0.45		4.6–5.6	(Chakraborty et al. 2007)
Termite mound	13.50	0.2 g/100 mL	3–10	(Fufa et al. 2014)
Modified beidellite and zeolite	0.476-0.841		4–11	(Bektaş et al. 2011)
Red mud	0.51		2.3	(Altundogan et al. 2000)
Kaolinite	0.86	4 g/100 mL	5	(Mohapatra et al. 2007)
Illite	0.52	4 g/100 mL	5	(Mohapatra et al. 2007)
Montmorillonite	0.64	4 g/100 mL	5	(Mohapatra et al. 2007)
Quartz tuff (Qz)	0.42	2 g/100 mL	3.5	This study
Stellerite tuffs (STL)	0.23	2 g/100 mL	3.5	This study
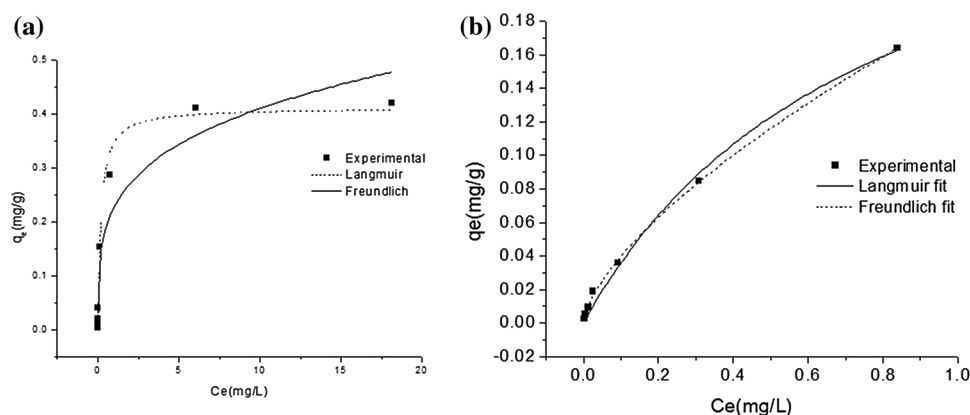
Fig. 10 Equilibrium sorption isotherms for As(V) removal using Qz (**a**) and STL (**b**) (conditions: temperature 25 ± 2 °C, adsorbent dose 20 g/L; initial pH 3.50; contact time 24 h, and shaking speed 200 rpm)
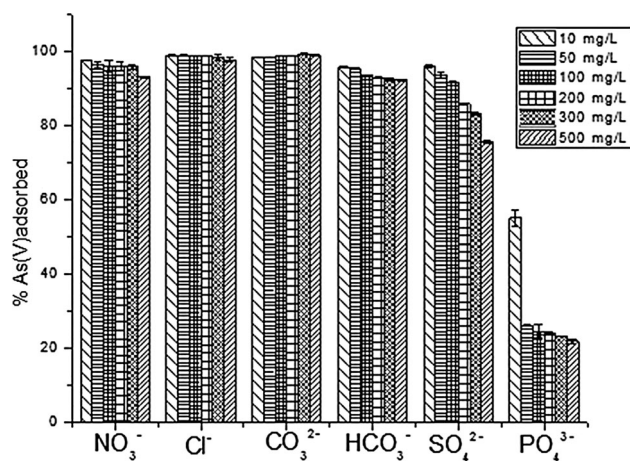
Fig. 11 Effect of co-occurring ions on the efficiency of As(V) removal (conditions: adsorbent Qz, 2 mg/L As(V), pH 3.50, equilibration time 24 h, temperature 25 ± 2 °C, adsorbent dose 20 g/L, and shaking speed 200 rpm)

aqueous solutions, respectively. It was noted that Qz was found better suited for As(V) removal than STL. Further, sequential extraction of As(V)-loaded adsorbents showed that the adsorption was due to the presence of short-range ordered and hydrous oxides of iron and aluminum. The results of this study showed that the mechanism of sorption was also well influenced with final pH of the solution. The buffering capacities of Qz and STL brought the solution pH, after sorption, to pH 5.76 and 5.40, respectively, from the initial working pH of 3.5.

References

Altundogan HS, Altundogan S, Tumen F, Bildik M (2000) Arsenic removal from aqueous solutions by adsorption on red mud. Waste Manag 20:761–767. doi:10.1080/10934520601187658

Amini M, Abbaspour KC, Berg M, Winkel L, Hug SJ, Hoehn E, Yang H, Johnson CA (2008) Statistical modeling of global geogenic arsenic contamination in groundwater. Environ Sci Technol 42:3669–3675. doi:10.1021/es702859e

Ayoob S, Gupta AK (2009) Performance evaluation of alumina cement granules in removing fluoride from natural and synthetic waters. Chem Eng J 150:485–491. doi:10.1016/j.cej.2009.01.038

Bektaş N, Aydın S, Öncel MS (2011) The Adsorption of Arsenic Ions Using Beidellite, Zeolite, and Sepiolite Clays: A Study of Kinetic, Equilibrium and Thermodynamics. Sep Sci Technol 46:1005–1016. doi:10.1080/01496395.2010.534524

Berg M, Tran HC, Nguyen TC, Pham HV, Schertenleib R, Giger W (2001) Arsenic contamination of groundwater and drinking water in Vietnam: a human health threat. Environ Sci Technol 35:2621–2626. doi:10.1021/es010027y

Bogdanov B, Georgiev D, Angelova K, Yaneva K (2009) Natural zeolites: clinoptilolite review. In: Economics and Society development on the Base of Knowledge. p 6

Borah D, Senapati K (2006) Adsorption of Cd(II) from aqueous solution onto pyrite. Fuel 85:1929–1934. doi:10.1016/j.fuel.2006.01.012

Brown GE, Henrich V, Casey W, Clark D, Eggleston C, Carrick Felmy A, Goodman Wayne D, Gratzel Michael, Gary McCarthy, Maureen I, Nealson Kenneth H, Sverjensky Dimitri, Toney Zachara, John M (1999) Metal oxide surfaces and their interactions with aqueous solutions and microbial organisms. Chem Rev 99:77–174

Chakraborty S, Wolthers M, Chatterjee D, Charlet L (2007) Adsorption of arsenite and arsenate onto muscovite and biotite mica. J Colloid Interface Sci 309:392–401. doi:10.1016/j.jcis.2006.10.014

Chowdhury SR, Yanful EK (2010) Arsenic and chromium removal by mixed magnetite–maghemite nanoparticles and the effect of phosphate on removal. J Environ Manag 91:2238–2247. doi:10.1016/j.jenvman.2010.06.003

Chutia P, Kato S, Kojima T, Satokawa S (2009a) Arsenic adsorption from aqueous solution on synthetic zeolites. J Hazard Mater 162:440–447. doi:10.1016/j.jhazmat.2008.05.061

Chutia P, Kato S, Kojima T, Satokawa S (2009b) Adsorption of As(V) on surfactant-modified natural zeolites. J Hazard Mater 162:204–211. doi:10.1016/j.jhazmat.2008.05.024

Da Silva YJAB, Do Nascimento CWA, Biondi CM (2014) Comparison of USEPA digestion methods to heavy metals in soil samples. Environ Monit Assess 186:47–53. doi:10.1007/s10661-013-3354-5

Flora SJS (2015) Arsenic: chemistry, occurence, and exposure. In: Flora SJS (ed) Handbook of arsenic toxicology, New York, p 752

Fufa F, Alemayehu E, Lennartz B (2013) Defluoridation of groundwater using termite mound. Water Air Soil Pollut 224:1552. doi:10.1007/s11270-013-1552-y

Fufa F, Alemayehu E, Lennartz B (2014) Sorptive removal of arsenate using termite mound. J Environ Manag 132:188–196

Fuller CC, Davis JA, Waychunas GA (1993) Surface chemistry of ferrihydrite: part 2. Kinetics of arsenate adsorption and coprecipitation. Geochim Cosmochim Acta 57:2271–2282. doi:10.1016/0016-7037(93)90568-H

Getaneh W, Alemayehu T (2006) Metal contamination of the environment by placer and primary gold mining in the Adola region of southern Ethiopia. Environ Geol 50:339–352. doi:10.1007/s00254-006-0213-5

Gómez-hortigüela L, Pinar AB, Pérez-pariente J, Sani T, Chebude Y, Díaz I (2014) Microporous and mesoporous materials ion-exchange in natural zeolite stilbite and significance in defluoridation ability. Microporous Mesoporous Mater 193:93–102. doi:10.1016/j.micromeso.2014.03.014

Guo H, Stüben D, Berner Z (2007) Removal of arsenic from aqueous solution by natural siderite and hematite. Appl Geochemistry 22:1039–1051. doi:10.1016/j.apgeochem.2007.01.004

Hall A (1998) Zeolitization of volcaniclastic sediments; the role of temperature and pH. J Sediment Res 68:739–745. doi:10.2110/jsr.68.739

Hall GEM, Pelchat JC, Gauthier G (1999) Stability of inorganic arsenic (III) and arsenic (V) in water samples. J Anal At Spectrom 14:205–213. doi:10.1039/a807498d

İnel O, Tümsek F (2000) The measurement of surface areas of some silicates by solution adsorption. Turk J Chem 24:9–19

Kallay N (2000) Interfacial dynamics: a surface science series. Marcel, Dekker inc, New York

Katsoyiannis IA, Zouboulis AI (2004) Application of biological processes for the removal of arsenic from groundwaters. Water Res 38:17–26. doi:10.1016/j.watres.2003.09.011

Kim EJ, Yoo JC, Baek K (2014) Arsenic speciation and bioaccessibility in arsenic-contaminated soils: sequential extraction and mineralogical investigation. Environ Pollut 186:29–35. doi:10.1016/j.envpol.2013.11.032

Langmuir I (1918) The adsorption of gases on plane surfaces of glass, mica and platinum. J Am Chem Soc 40:1361–1403

Li Q, Xu XT, Cui H, Pang J, Wei Z, Sun Z (2012) Comparison of two adsorbents for the removal of pentavalent arsenic from aqueous solutions. J Environ Manag 98:98–106. doi:10.1016/j.jenvman.2011.12.018

Manning B, Goldberg S (1996) Modeling competitive adsorption of arsenate with phosphate and molybdate on oxide minerals. Soil Sci Soc Am J 60:121. doi:10.2136/sssaj1996.03615995006000010020x

Masscheleyn PH, Delaune RD, Patrick WH Jr (1991) Effect of redox potential and ph on arsenic speciation and solubility in a contaminated soil. Environ Sci Technol 25:1991

Mketo N, Nomngongo PN, Ngila JC (2015) A rapid microwave-assisted acid extraction method based on the use of diluted HNO_3-H_2O_2 followed by ICP-MS analysis for simultaneous determination of trace elements in coal samples. Int J Environ Anal Chem 95:37–41. doi:10.1080/03067319.2015.1025226

Mohan D, Pittman CU (2007) Arsenic removal from water/wastewater using adsorbents–a critical review. J Hazard Mater 142:1–53

Mohapatra D, Mishra D, Chaudhury GR, Das RP (2007) Arsenic(V) adsorption mechanism using kaolinite, montmorillonite and illite from aqueous medium. J Environ Sci Heal Part A Toxic/Hazard Subst Environ Eng 4:463–469. doi:10.1080/10934520601187666

Rango T, Bianchini G, Beccaluva G, Tassinari R (2010) Geochemistry and water quality assessment of central main ethiopian rift natural waters with emphasis on source and occurrence of fluoride and arsenic. J Afr Earth Sci 57:479–491

Rango T, Vengosh A, Dwyer G, Bianchini G (2013) Mobilization of arsenic and other naturally occurring contaminants in groundwater of the Main Ethiopian Rift aquifers. J water Res 47:1–18

Ruggieri F, Marín V, Gimeno D et al (2008) Application of zeolitic volcanic rocks for arsenic removal from water. Eng Geol 101:245–250. doi:10.1016/j.enggeo.2008.06.006

Shan C, Tong M (2013) Efficient removal of trace arsenite through oxidation and adsorption by magnetic nanoparticles modified with Fe-Mn binary oxide. Water Res 47:3411–3421. doi:10.1016/j.watres.2013.03.035

Shevade S, Ford RG (2004) Use of synthetic zeolites for arsenate removal from pollutant water. Water Res 38:3197–3204. doi:10.1016/j.watres.2004.04.026

Smith AH, Elena OL, Rahman M (2000) Contamination of drinking-water by arsenic in Bangladesh: a public health emergency. Bull World Health Organ 78:1093–1103

Sverjensky DA, Fukushi K (2006) Anion adsorption on oxide surfaces: inclusion of the water dipole in modeling the electrostatics of ligand exchange. Environ Sci Technol 40:263–271. doi:10.1021/es051521v

Tadesse S (2009) Mineral Resources Potential of Ethiopia

Taubaso C, Dos Santos Afonso M, Torres Sánchez RM (2004) Modelling soil surface charge density using mineral composition. Geoderma 121:123–133. doi:10.1016/j.geoderma.2003.11.005

Weber TW, Chakravorti RK (1974) Pore and solid diffusion models for fixed-bed adsorbers. AIChE J 20:228–238. doi:10.1002/aic.690200204

Weil J (1984) A review of electron spin spectroscopy and its application to the study of paramagnetic defects in crystallin quartz. Phys Chem Miner 10:149–165

Wenzel WW, Kirchbaumer N, Prohaska T et al (2001) Arsenic fractionation in soils using an improved sequential extraction procedure. Anal Chim Acta 436:309–323

Xu H, Allard B, Grimvall A (1988) Influence of pH and organic substance on the adsorption of As(V) on geologic materials. Water Air Soil Pollut 40:293–305. doi:10.1007/BF00163734

Xu YH, Nakajima T, Ohki A (2002) Adsorption and removal of arsenic(V) from drinking water by aluminum-loaded Shirasu-zeolite. J Hazard Mater 92:275–287. doi:10.1016/S0304-3894(02)00020-1

Zeng L (2004) Arsenic adsorption from aqueous solutions on an Fe(III)-Si binary oxide adsorbent. Water Qual Res J Canada 39:267–275

Zhang W, Pritam S, Paling E, Delides S (2004) Arsenic removal from contaminated water by natural iron ores. Miner Eng 17:517–524

Zhu H, Jia Y, Wu X, Wang H (2009) Removal of arsenic from water by supported nano zero-valent iron on activated carbon. J Hazard Mater 172:1591–1596. doi:10.1016/j.jhazmat.2009.08.031